JACS
JOURNAL OF THE AMERICAN CHEMICAL SOCIETY
pubs.acs.org/JACS
Article

Ultrafast Dynamics and Vibrational Relaxation in Six-Coordinate Heme Proteins Revealed by Femtosecond Stimulated Raman Spectroscopy

Carino Ferrante,[⊥] Giovanni Batignani,*[,⊥] Emanuele Pontecorvo,[⊥] Linda C. Montemiglio, Marten H. Vos, and Tullio Scopigno*

Cite This: J. Am. Chem. Soc. 2020, 142, 2285−2292
Read Online
ACCESS | Metrics & More | Article Recommendations | Supporting Information

ABSTRACT: Identifying the structural rearrangements during photo-induced reactions is a fundamental challenge for understanding from a microscopic perspective the dynamics underlying the functional mechanisms of heme proteins. Here, femtosecond stimulated Raman spectroscopy is applied to follow the ultrafast evolution of two different proteins, each bearing a six-coordinate heme with two amino acid axial ligands. By exploiting the sensitivity of Raman spectra to the structural configuration, we investigate the effects of photolysis and the binding of amino acid residues in cytochrome *c* and neuroglobin. By comparing the system response for different time delays and Raman pump resonances, we show how detailed properties of atomic motions and energy redistribution can be unveiled. In particular, we demonstrate substantially faster energy flow from the dissociated heme to the protein moiety in cytochrome *c*, which we assign to the presence of covalent heme−protein bonds.

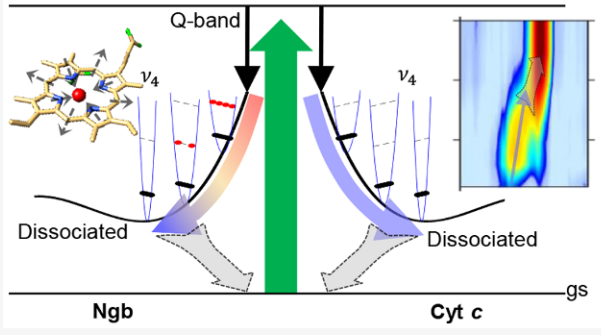

INTRODUCTION

Heme proteins constitute one of the most important families of macromolecular compounds, being present in all living organisms and displaying a wide range of biological functions, including oxygen transport and intracellular trafficking. The heme protein's core is an iron atom confined in a porphyrin ring via four bonds with nitrogen atoms and able to bind two axial ligands. One of these ligands is usually an amino acid as a histidine or a methionine. The other ligation site can be occupied by a small gaseous molecule such as O_2 or CO or by another amino acid, or it can be unoccupied. Changes in the ligation state are often involved in the function of the heme protein. Therefore, the characterization of the heme−iron bonds and their connection with conformational rearrangements of the porphyrin are crucial for understanding the structural mechanisms ruling the biological role of such prototypical compounds. Notably, several concurring processes, such as structural reconfiguration, energy redistribution and the relaxations of intermediate excited states, occur on picosecond and femtosecond time scales, and can be accompanied by bond breaking and recombination events. The advent of femtosecond laser sources and the development of optical nonlinear techniques have paved the way for a direct exploration of heme protein ultrafast dynamics.[1−5]

Within such studies, particular effort has been devoted to the understanding of a rapidly expanding group of proteins, namely, those able to form the iron atom's sixth bond either with an internal residue or with an external ligand (such as O_2, NO, or CO). Notably, within this class of proteins, the exchange of internal and external ligands is often thought to be functional. Upon (photo)dissociation of a gaseous ligand, the kinetics of binding of the internal residue is rate-limited by the migration of the gaseous ligand through the protein matrix and steric rearrangement,[6−13] whereas the dissociation of the heme-residue bond in the absence of external ligands leads to at least 6 orders of magnitude faster rebinding.[14−16]

In particular, the photodissociation and fast rebinding dynamics of the heme-residue bond, occurring on the picosecond time scale (5−9 ps), have been assessed using transient absorption (TA) spectroscopy.[17,18] Critically, due to its lack of structural sensitivity, TA is able neither to directly monitor heme geometrical rearrangements nor to distinguish between transient electronic intermediates or de-excitation to a vibrationally hot electronic ground state.[4,19−21] In contrast, conventional spontaneous time-resolved resonance Raman (TR^3) spectroscopy can provide direct information on transient structural configurations of a reacting heme by accessing its vibrational fingerprints. However, for TR^3 the

Received: October 1, 2019
Published: January 9, 2020

https://dx.doi.org/10.1021/jacs.9b10560
J. Am. Chem. Soc. 2020, 142, 2285−2292

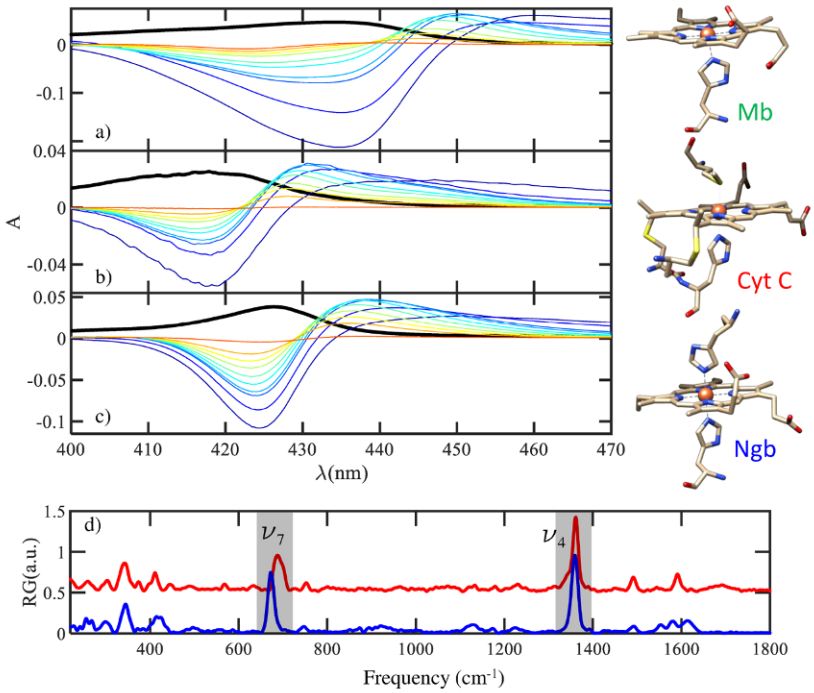

Figure 1. TA traces around the Soret band for different time delays in (a) Mb, (b) cyt *c*, and (c) Ngb are reported as colored lines. The time delays are 0.1, 0.3, 0.5, 1, 2, 3, 5, 7, 10, and 30 ps from blue to red. The scaled static absorption profiles are reported as black lines. (d) cyt *c* and Ngb static stimulated Raman spectra, measured with the RP tuned to 430 nm (red and blue lines, respectively). The two main peaks at ∼700 and ∼1350 cm^{-1} correspond to totally symmetric in-plane breathing modes of the porphyrin ring and are conventionally referred to as the ν_7 and ν_4 bands, respectively.

temporal and energy resolutions are fundamentally constrained by the Fourier transform limit ($\Delta E \Delta t \geq 15$ cm^{-1} ps), making it difficult to resolve spectral details arising from ultrafast dynamics on the subpicosecond time scale. Nevertheless, using an accurate balance of the two resolutions, Cianetti et al. provided useful insight on the photolysis by observing the appearance, in ferrous six-coordinate (6-c) cytochrome *c* (cyt *c*), of a low-frequency Raman band (centered at 216 cm^{-1} and assigned to the iron-histidine stretching mode) sensitive to the doming of the porphyrin ring on the picosecond time scale.[22]

In this work, in order to circumvent the TR^3 limitations, we take advantage of the recently introduced femtosecond stimulated Raman spectroscopy (FSRS) nonlinear technique[23−25] combining both high spectral and temporal resolutions.[26−31] The experimental scheme requires three pulses: a femtosecond actinic pump (AP) that triggers the dynamics of interest, a Raman pulse (RP), and a broadband probe pulse (PP) whose joint action coherently stimulates and records Raman oscillations, providing the chance to follow photoreactions with uncompromised temporal precision (down to 50 fs) and spectral resolution (a few wavenumbers).[24] Specifically, by probing transient stimulated vibrational spectra and taking advantage of the wavelength tunability of a narrow-band Raman pulse,[32,33] FSRS has proven able to assign contributions arising from different intermediate states and to provide important insights on femtosecond structural changes upon photoexcitation.[34−40] By comparing the Raman band cross sections and positions measured by scanning the RP wavelength across the absorption bands of transient and relaxed species,[41,42] it is possible to extract detailed structural information on the system's dynamics. For this reason, we developed a FSRS setup with a tunable Raman pulse (femtosecond stimulated resonance Raman scattering, FSRRS) that is able to explore resonance effects across the Soret absorption band (400−460 nm).[43] Here we study two heme proteins with the hemes in the ferrous 6-c form with two amino acid ligands, namely, cyt *c* and neuroglobin (Ngb). Ngb is a relatively recently discovered protein,[44] which is present predominantly in brain and nerve tissues, and its biological function is still elusive. As the prototypical oxygen-storage protein myoglobin (Mb), it can easily bind small gaseous ligands to the *b*-type heme cofactor, but whereas in unliganded deoxy-myoglobin the heme is 5-c, in the absence of external ligands in Ngb it is 6-c with two histidine residues as ligands. Cyt *c* is a ubiquitous and well-studied soluble electron-transfer heme protein. During its electron-transfer function, it switches between the ferric and ferrous states, always remaining 6-c with histidine and methionine as axial ligands. Other than globin heme proteins, it does not readily bind external ligands except when it is modified by interactions with lipids.[45,46] It is also relatively rigid,[47,48] a property thought to be favorable to its electron-transfer function.[49] Another important difference with Ngb is that it carries a *c*-type heme, which implies that the heme binds to the protein not only via the iron atom but also via two covalent bonds of the peripheral vinyl groups with cysteine residues.[50] The external ligand[51] and one of the internal ligands in ferrous 6-c heme proteins not binding external ligands[18] can be photodissociated with a high quantum yield.

Our Raman results elucidate the details of the dynamics for the photoexcitation in Ngb and cyt *c*, allowing us to discern between structural modification and energy transfer in such molecules. Specifically, we find a new marker of internal ligand photolysis in the high-frequency region (ν_4 at ∼1360 cm^{-1}) common to both systems and protein-specific cooling processes that involve different Raman modes.

https://dx.doi.org/10.1021/jacs.9b10560
J. Am. Chem. Soc. 2020, 142, 2285−2292

RESULTS

To visualize the electronic resonances of the system, TA spectra of photoexcited ferrous Mb (5-c), cyt *c*, and Ngb are reported in Figure 1, with a sketch of the heme pockets for the three different protein species reported in the right panel. Notably, in view of the lack of photolysis due to the absence of an axial distal ligand, the photodynamics of the 5-c heme in Mb is in principle different from that of 6-c hemes and is characterized, for times >50 fs, only by energy transfer.[20,42] Although the structural pathway is different, the TA spectra recorded in the Soret band are qualitatively similar and characterized by a dispersive line shape, with an absorption maximum that is red-shifted with respect to the Soret band, testifying to the poor structural sensitivity of TA.

Specifically, as quantitatively evaluated in Figure 1a–c, after the instantaneous appearance of a dispersive feature in TA data, the recovery of the initial absorption profile occurs faster in Mb (~3 ps) with respect to the case of the two 6-c hemes (~8 ps for Ngb and ~5 ps for cyt *c*; cf. refs 18 and 21).

A careful inspection of the TA spectra also reveals the presence of a subpicosecond more red-shifted tail, possibly related to the heating effects. This relaxation is present for all three investigated species,[16,18,52] and it occurs on the femtosecond time scale (from ~150 fs in cyt *c* to ~400 fs in Ngb and Mb).

Steady-state stimulated Raman spectra of cyt *c* and Ngb, recorded without the AP by tuning the RP to be in resonance with the Soret band absorption setup, are also reported in Figure 1d and reveal two dominant modes (ν_7 and ν_4) corresponding to totally symmetric in-plane breathing modes of the porphyrin ring.

Cytochrome *c*. The FSRRS measurements of cyt *c* offer a direct way to follow the molecular dynamics. The experimental data, reported in Figure 2, show two main features: (i) a shift in the ν_4 position from 1360 to ~1342 cm^{-1} occurring on the time scale of a few picoseconds and (ii) a shift of the vibrational modes up to 700 cm^{-1} to lower energy; such a shift is more pronounced for higher RP wavelengths. This latter effect, which is more evident during the first 1 ps, can be attributed to the out-of-equilibrium heating of vibrational modes[17] corresponding to an increase in the population of vibrationally excited states. This implies the appearance in the Raman spectrum of hot bands, i.e., Raman transitions from vibrationally excited levels ($n > 0$) to the higher ones ($n + 1$). Hot bands are generally centered at lower wavenumbers with respect to the fundamental bands ($0 \rightarrow 1$) due to anharmonic molecular potentials (a further discussion is reported in the SI), and they are more pronounced for RP wavelengths which are red-shifted with respect to the Soret band maximum.[42] In striking contrast, the 1342 cm^{-1} band, still red-shifted with respect to the unphotoexcited ν_4 ground-state peak (~1360 cm^{-1}), cannot be ascribed to a hot band of the 6-c heme ground state because it does not undergo an amplitude enhancement for red-shifted RP wavelengths at any of the monitored time delays. Furthermore, the picosecond (~1360 cm^{-1}) band is weaker than the shifted peak also in resonance with the vibrational ground state of the 6-c configuration (at RP = 430 nm). Since the population of the $n = 1$ level cannot be larger than that of the $n = 0$ level, the recorded FSRRS spectra are not compatible with a thermal distribution of ν_4 vibrational levels. Moreover, the time-dependent central frequency of the red-shifted 1342 cm^{-1} band, reported in

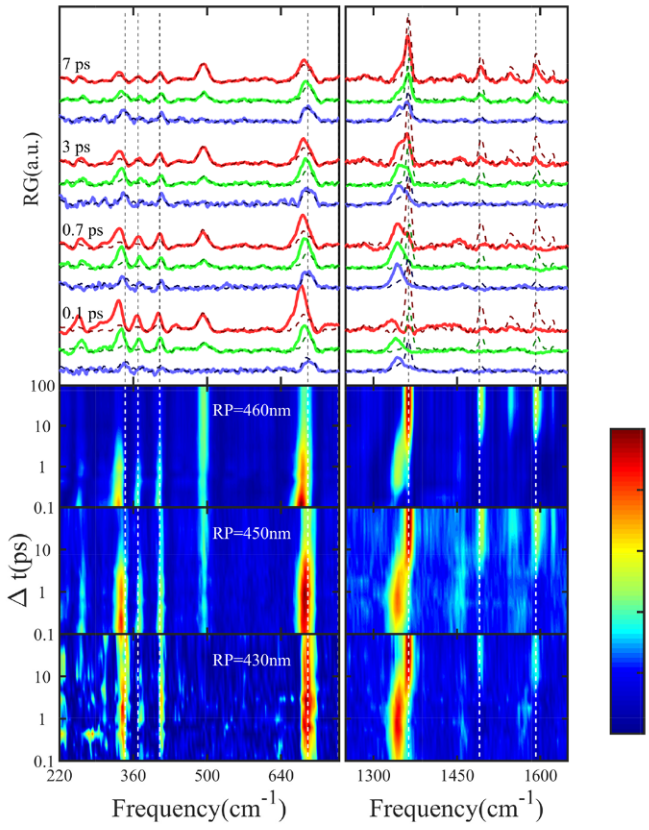

Figure 2. (Top) FSRRS spectra of ferrous cyt *c* (solid lines) are shown for selected time delays with the RP at 460 (red), 450 (green), and 430 (blue). Reference spectra in the absence of the AP are also reported as dashed lines. (Bottom) Corresponding FSRRS color maps are reported for all of the measured time delays from 0.1 to 100 ps. The vertical dashed lines are guides to the eye. The unphotoexcited contribution has been removed, and probe chirp temporal shifts have been corrected.

Figure 3 (red circles connected by a dashed line), cannot be ascribed to a hot band population, which would show a time-independent energy difference between the vibrational levels, being rather compatible with an evolution in an out-of-equilibrium configuration (as clarified below).

Considering the recombination time scale of the residue binding,[14,17] the spectrally resolved transient 1340–1350 cm^{-1} ν_4 peak can be assigned to the methionine-photodissociated 5-c heme. Consequently, hereafter we will refer to the two contributions as the ground state and the photodissociated state (ν_4^{gs} and ν_4^{pd}, respectively).

Interestingly, a similar measurement was performed with TR^3,[16] where the ν_4 band shift occurring on the picosecond time scale was interpreted as vibrational cooling related to anharmonic coupling of the ν_4 band to lower-frequency modes. We note that the time constant of the shift was found to be somewhat shorter in the present FSRS work (2.8 ps) than in the TR^3 experiments (6.8 ps). This difference is presumably related to the much lower TR^3 spectral resolution, which leads to uncertainty in distinguishing the two ν_4 contributions.

Neuroglobin. The FSRRS spectra of photoexcited ferrous Ngb, measured with the RP tuned to 460 nm, are reported in Figure 4 and at first sight show trends similar to those recorded for the cyt *c* case. In particular, down-shifts of the vibrational modes up to 700 cm^{-1} are measured on the picosecond time scale and are due to the heating and subsequent cooling

https://dx.doi.org/10.1021/jacs.9b10560
J. Am. Chem. Soc. 2020, 142, 2285–2292

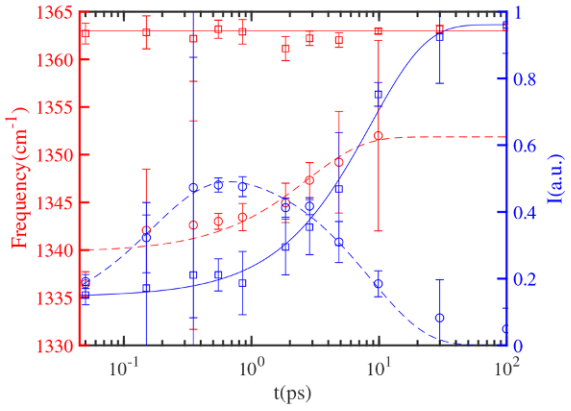

Figure 3. Intensity (blue right axis) and frequency (red left axis) of ν_4^{gs} (squares) and ν_4^{pd} (circles) bands, extracted with the RP tuned to 450 nm, are reported as a function of the pump−probe delay. Time-dependent amplitudes and positions are extracted by fitting the experimental spectra with Gaussian profiles. The ν_4^{pd} position is not reported for time delays with vanishing ν_4^{pd} intensity. The recovery of the ν_4^{gs} peak amplitude occurs simultaneously with the disappearance of ν_4^{pd}, which shows an ∼10 cm^{-1} frequency shift (red dashed line). The kinetics of the relaxation process are obtained by mono- and biexponential fits of peak amplitudes and positions (reported as lines). Specifically, the extracted time scales are 0.18 and 8.6 ps for the ν_4^{pd} intensity, 8.6 ps for the ν_4^{gs} intensity, and 2.8 ps for the ν_4^{pd} peak position.

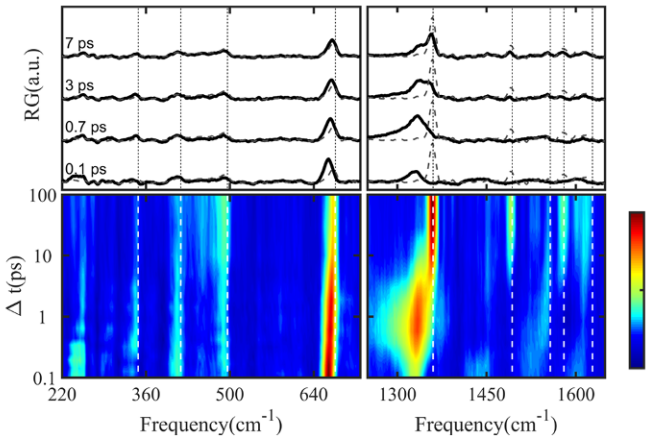

Figure 4. FSRRS spectra of ferrous Ngb (solid lines) are shown for selected time delays. (Top) Reference spectra in the absence of the actinic pulse are reported as dashed lines. (Bottom) Corresponding FSRRS color maps are reported for all of the measured time delays from 0.1 to 100 ps. The vertical dashed lines are guides to the eye. The RP wavelength is set at 460 nm, the unphotoexcited contribution has been removed, and probe chirp temporal shifts have been corrected.

processes. In parallel, the transient ν_4^{pd} mode exhibits rich dynamics occurring within the first 10 ps. In particular, the ν_4^{pd} band has an asymmetric line shape with a red-shifted tail. (See the solid line at 0.7 ps in Figure 4.)

To understand the origin of this contribution, we compare the same measurement at a 1 ps time delay (when the ν_4^{gs} contribution is negligible) scanning different RP wavelengths across the red side of the Soret absorption band, as shown in Figure 5. A large dependence of the red-shifted tail as a function of the RP wavelength is observed, as expected, within a hot bands scenario.[42] Moreover, the broad bandwidth of this contribution (∼50 cm^{-1}, highlighted by the red area in Figure 5) indicates the lifetime of the first vibrationally excited state to be much shorter than that of the ground state.

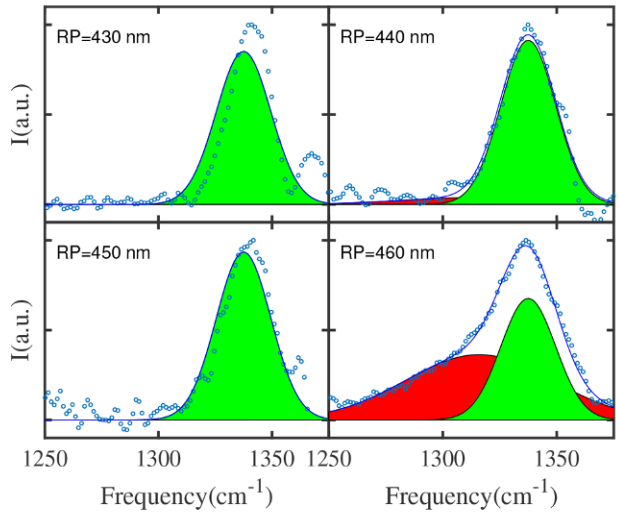

Figure 5. FSRRS ν_4 spectra of ferrous Ngb (blue circles), after subtraction of the nonexcited molecular fraction, at 1 ps for different RP wavelengths. For this time delay, the experimental data can be fitted (blue line) as the sum of two Gaussian contributions that represent the fundamental ν_4^{pd} peak (green area) and its first hot band (red area). The contribution of the ν_4^{gs} band is negligible for this time delay. In agreement with ref 42, the hot-band contribution is emphasized for the 460 nm (red-shifted) RP wavelength.

Moreover, the peak positions of the fundamental ν_4^{pd} peak and its first hot band, reported in Figure 6, have a similar trend

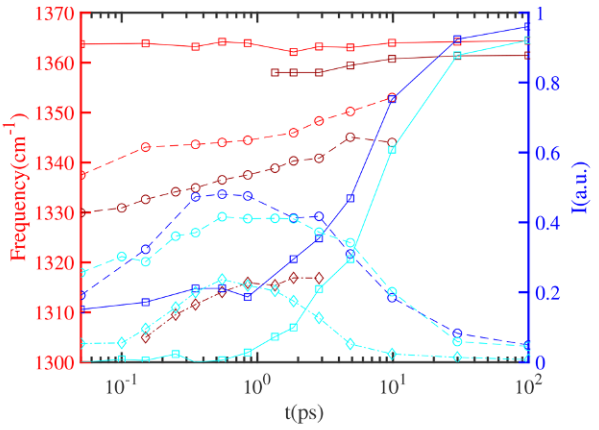

Figure 6. Intensity of cyt *c* (blue lines) and Ngb (cyan lines) and frequency of cyt *c* (red lines) and Ngb (brown lines) of ν_4^{gs} (squares), ν_4^{pd} (circles), and hot bands of ν_4^{pd} (diamonds) reported for different time delays. Time-dependent amplitudes and positions are extracted from fitting the experimental spectra with Gaussian profiles. The peak position is reported only for intensity $I(t)$ larger than $0.08I(-10$ ps). The recovery of the ν_4^{gs} intensity is simultaneous with the disappearance of ν_4^{pd}, which has a frequency shift (red dashed line) of ∼10 cm^{-1}.

and, consequently, a constant difference of ∼25 cm^{-1}. This implies that during the structural evolution in the photodissociated state the anharmonicity factor, α, is almost constant. Assuming a Morse potential, in Ngb, $\alpha \approx 0.0088$ (SI) is 2 times larger than the value extracted for myoglobin ($\alpha = 0.004$).[42]

https://dx.doi.org/10.1021/jacs.9b10560
J. Am. Chem. Soc. 2020, 142, 2285−2292

In summary, Ngb shows a Raman signature of the photodissociated state, in this case arising from the photolysis of the histidine,[18] with a transient hot ν_4^{pd} vibrational state that decays on the picosecond time scale, analogous to the case of excited deoxy Mb[42] (SI). This latter feature represents an important difference with respect to the cyt *c* case that does not show this heating of the ν_4^{pd} vibrational mode.

DISCUSSION

In the literature, the photolysis of amino acid residues, i.e., histidine and methionine, from ferrous hemes has been mainly investigated with TA spectroscopy.[14,17,18,53−56] The only Raman evidence of bond breaking, obtained with a picosecond time resolution by spontaneous TR^3, is the appearance in cyt *c* of the iron−histidine band,[22] following vibrational coherence spectroscopy assignments.[17] Vibrational cooling subsequent to photolysis has been studied on the picosecond time scale by TR^3, but here the poor spectral and temporal resolution limit the obtainable information on the evolution of the dissociated configuration and in particular does not allow us to resolve hot bands. On the contrary, FSRRS transient spectra are able to unveil and track a novel marker of photolysis in the ν_4 high-frequency region. Moreover, FSRRS high spectral and temporal resolutions enabled us to disclose marked differences in the structural dynamics and energy flow in the investigated *b*- and *c*-type hemes. The results are summarized in Figure 7.

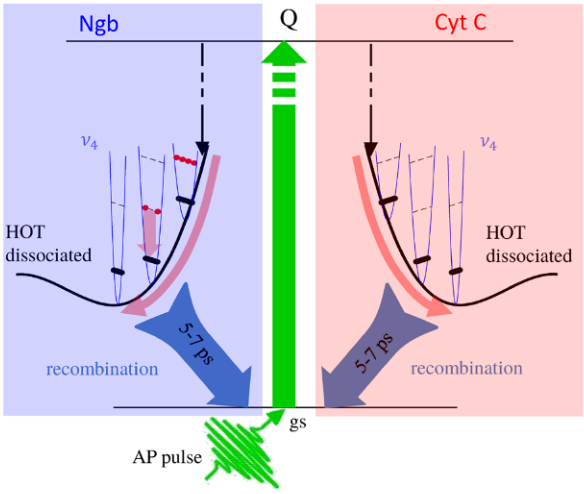

Figure 7. Interaction with the AP pulse promotes the system from the ground state to the Q band in both 6-c molecules. The system decays instantaneously (<50 fs) into the hot photodissociated states of Ngb (blue area) and cyt *c* (red area), in which the internal residue (histidine for Ngb and methionine for cyt *c*) is detached from the iron atom. Under this condition, a cooling process and a structural relaxation can be observed. The observation of the first ν_4^{pd} hot band testifies to the population of vibrational excited states in Ngb (red circles in the ν_4 potential). The last step is the recovery of the ground state in 5−9 ps with the binding of the residue.

Structural Dynamics. As shown in Figure 6, similar dynamics are observed for the frequency position of ν_4^{gs} and ν_4^{pd} bands in the two 6-c heme−protein complexes investigated in this work. In particular, after an instantaneous softening of the ν_4^{pd} mode, a partial recovery (on a 2.8 ps time scale) toward the gs frequency is observed before full relaxation to the 6-c ground state. This recovery, quantified in Figure 3, can be interpreted in two different ways: anharmonic mode coupling with a low frequency mode[4] or a picosecond geometrical reorganization able to accommodate the recombination of the distal ligand after its instantaneous photolysis.[39] Notably, the observation of the ν_4^{pd} hot band only for the Ngb case suggests ν_4 coupling that is different for the two 6-c systems,[42] which would imply different trends for the two 6-c proteins (not observed) in the presence of a ν_4^{pd} peak shift due to anharmonic coupling. Moreover, in striking contrast to the ν_4^{pd} dynamics measured in deoxy Mb[42] and in CO-bound Mb,[57] where the ν_4 anharmonic coupling induces an initial ∼4 cm^{-1} peak red shift followed by recovery, the ν_4^{pd} peak measured in both 6-c molecules shows a strong (>10 cm^{-1}) and monotonic (in time) blue shift (a direct comparison is provided in Figure S2 of the SI). Taken together, these results point to the presence of a picosecond geometrical reorganization. This indicates that such sensitivity of the ν_4 vibrational coordinate to the system structural reconfiguration is a general feature in the process of bond breaking/reformation of the ferrous heme with an internal residue. Within this context, the binding to an amino acid, which is part of the protein backbone, is suggestive of a larger heme distortion with respect to the case of small gaseous ligands, which would eventually lead to stronger reorganization upon bond dissociation. Interestingly, a strong ruffling deformation due to the heme−protein interactions has been invoked for (oxidized) cytochrome *c*, with the (very low frequency) ruffling mode typically dampening within a few picoseconds.[58]

Energy Flow. The hot band dynamics, observed in the two 6-c systems, show an out-of-equilibrium energy distribution in the photodissociated intermediate state, with a key role of the vibrational modes up to 700 cm^{-1}, as in the case of 5-c Mb.[42] Specifically, these hot bands are the signature of a high-temperature distribution of vibrational excited states and appear in less than 100 fs, testifying to the crucial role of these modes as thermal receptors. Moreover, the picosecond recovery of the cold state highlights their efficiency in the flow of thermal energy out of the heme via coupling to low-frequency (delocalized) modes of the protein environment. The scenario is quite different for high-frequency modes and, specifically, for the ν_4 band. In the case of 5-c Mb, picosecond trapping of thermal energy in the $n = 1$ level of the ν_4 mode is observed. Starting from 6-c heme systems, a 5-c hot heme state is also populated, albeit with less vibrational energy due to the energy required to dissociate the Fe−residue bond, and the dynamics are complicated by the photolysis process. The photodissociated Ngb shows a very prominent ν_4 hot band, similar to the Mb case. In striking contrast, in cyt *c* no population of higher ν_4 vibrational levels is observed on the same time scale. These results indicate that either these levels do not get significantly populated from the initial broad manifold of vibrational states[42] or that they very rapidly (<100 fs) decay to the $n = 0$ level. Notably, this observation implies a more efficient cooling process in cyt *c* than in Ngb, also providing a rationale for the faster dynamics of the red tail measured by TA in cyt *c* (∼150 fs) with respect to the Ngb spectra (∼400 fs). We assign this striking difference between cyt *c* and Ngb to the fact that the *c*-type heme is bound to the protein not axially only via the heme iron but also via two covalent bonds with cysteine residues at the periphery of the heme plane. Therefore, the effective coupling of the ν_4 in-plane mode to protein modes in the same frequency range will be much stronger, and energy redistribution with high-frequency protein modes is more efficient. Energy flow has been modeled

https://dx.doi.org/10.1021/jacs.9b10560
J. Am. Chem. Soc. 2020, 142, 2285−2292

in a number of heme proteins, and several works have been devoted to cyt *c*.[47,53,59−61] In comparison to similar studies on myoglobin,[59] it was indeed observed that through-bond energy flow plays a much stronger role in cyt *c*, in particular, by flow through the cross-linked cysteine residues, including on the 100 fs time scale.[62] In a different study, the cysteines were found to respond at a rate >500 ps^{-1} even when the excess energy was deposited initially only in close proximity to the heme iron.[61] These studies thus appear in qualitative agreement with the present experimental work. Mode-resolved theoretical analyses may allow a more detailed comparison with the FSRS data.

EXPERIMENTAL SECTION

Sample Preparation. Murine deoxy neuroglobin is prepared by dissolving the freeze-dried ferric form[63] in a phosphate buffer (pH 7.4), and the obtained solution is purified into a biochemical basket centrifuge. Sodium dithionite ($Na_2S_2O_4$) is used to reduce the ferric neuroglobin to its ferrous form. Protein was reduced in a nitrogen-purged buffer to avoid exposure to atmospheric oxygen. The concentrations of the samples are between 100 and 200 μM.

Horse-heart cyt *c* was purchased from Sigma and prepared as described above for neuroglobin.

The sample is allowed to flow anaerobically through the transmission cell during the experiment due to a peristaltic pump so as to guarantee a fresh sample at every laser shot (1 kHz). All Raman measurements were performed at room temperature. The transmission cell is mounted onto an upright motorized translator to allow regular movements to minimize window damage by the three beams.

FSRS Setup. A detailed description of our FSRRS setup has been given elsewhere.[32,43,64] The basic concept is to use an ∼1 μJ energy, 50 fs time-duration AP tuned to the heme Q band (550 nm) to photoexcite the system, triggering the dynamics of interest. The system evolution is then monitored by a couple of a narrow-band tunable Raman pulses (RPs), which provides the spectral resolution, and a broad-band femtosecond probe pulse (PP), which guarantees the time precision. The joint action of temporally and spatially overlapped RP and PP allows for recording stimulated Raman scattering (SRS) spectra, coherently generated on top of the highly directional PP and hence essentially free from the fluorescent background. Optical Kerr effect cross-correlation has been exploited to measure the arrival time of the different probe pulse spectral components[25,65] in order to correct for the probe chirp temporal shifts.[66] The TA measurements, recorded in absence of the RP, have been performed with the same pulse properties.

CONCLUSIONS

Tracking Raman bands dynamics in 6-c heme proteins with the high spectral and temporal resolutions provided by FSRRS allowed us to identify a new marker of photolysis related to a red-shifted contribution of the ν_4 mode, which was exploited to track the system relaxation. In addition, the dynamics of hot band contributions unveil the pathway of thermal relaxation in such macromolecules. In particular, we detected a high out-of-equilibrium condition in the photolyzed state consisting of a high temperature for low vibrational modes (up to 700 cm^{-1}). Interestingly, in Ngb but not in cyt *c*, a trapping of thermal energy in the $n = 1$ level is observed for the ν_4 vibrational coordinate. Such an effect presumably originates from the different heme bonding of these proteins and may be related to the difference in rigidity required for the respective small-molecule and electron-transfer functions of these proteins. After the recombination of the internal ligand, the systems are fully relaxed in the gs, without any residual thermal heating effect.

ASSOCIATED CONTENT

Supporting Information

The Supporting Information is available free of charge at https://pubs.acs.org/doi/10.1021/jacs.9b10560.

Anharmonicity factor extracted from the FSRRS spectra; comparison between five-coordinate (Mb) and six-coordinate (Ngb and cyt *c*) ν_4 peak dynamics (PDF)

AUTHOR INFORMATION

Corresponding Authors

Giovanni Batignani − *Dipartimento di Fisica, Università di Roma "La Sapienza", Rome I-00185, Italy;* orcid.org/0000-0002-6214-8604; Email: giovanni.batignani@uniroma1.it

Tullio Scopigno − *Dipartimento di Fisica, Università di Roma "La Sapienza", Rome I-00185, Italy; Center for Life Nano Science @Sapienza, Istituto Italiano di Tecnologia, Rome I-00161, Italy;* orcid.org/0000-0002-7437-4262; Email: tullio.scopigno@roma1.infn.it

Authors

Carino Ferrante − *Dipartimento di Fisica, Università di Roma "La Sapienza", Rome I-00185, Italy; Center for Life Nano Science @Sapienza, Istituto Italiano di Tecnologia, Rome I-00161, Italy;* orcid.org/0000-0002-6391-0672

Emanuele Pontecorvo − *Dipartimento di Fisica, Università di Roma "La Sapienza", Rome I-00185, Italy*

Linda C. Montemiglio − *Dipartimento di Scienze Biochimiche "Alessandro Rossi Fanelli", Università di Roma "La Sapienza", Rome I-00185, Italy*

Marten H. Vos − *LOB, Ecole Polytechnique, CNRS, INSERM, Institut Polytechnique de Paris, Palaiseau 91128, France;* orcid.org/0000-0003-0493-4831

Complete contact information is available at: https://pubs.acs.org/10.1021/jacs.9b10560

Author Contributions

⊥These authors contributed equally to this work

Notes

The authors declare no competing financial interest.

ACKNOWLEDGMENTS

The authors thank B. Vallone and the Dipartimento di Scienze Biochimiche and Istituto Pasteur-Fondazione Cenci Bolognetti of Università di Roma "La Sapienza" for the help with sample preparation. We acknowledge M. Brunori for many inspiring discussions. G.B. acknowledges the "Avvio alla ricerca 2018" grant by Sapienza Universitá di Roma. T.S. acknowledges the "Progetti di ricerca di Ateneo 2018" grant by Sapienza Universitá di Roma.

REFERENCES

(1) Mizutani, Y.; Kitagawa, T. Direct Observation of Cooling of Heme Upon Photodissociation of Carbonmonoxy Myoglobin. *Science* **1997**, *278*, 443−446.

(2) Rosca, F.; Kumar, A. T. N.; Ionascu, D.; Sjodin, T.; Demidov, A. A.; Champion, P. M. Wavelength selective modulation in femto-second pump−probe spectroscopy and its application to heme proteins. *J. Chem. Phys.* **2001**, *114*, 10884.

(3) Kholodenko, Y.; Volk, M.; Gooding, E.; Hochstrasser, R. Energy dissipation and relaxation processes in deoxy myoglobin after photoexcitation in the Soret region. *Chem. Phys.* **2000**, *259*, 71−87.

(4) Franzen, S.; Kiger, L.; Poyart, C.; Martin, J.-L. Heme Photolysis Occurs by Ultrafast Excited State Metal-to-Ring Charge Transfer. *Biophys. J.* **2001**, *80*, 2372−2385.
(5) Vos, M. H. Ultrafast dynamics of ligands within heme proteins. *Biochim. Biophys. Acta, Bioenerg.* **2008**, *1777*, 15−31.
(6) Kruglik, S. G.; Yoo, B.-K.; Lambry, J.-C.; Martin, J.-L.; Negrerie, M. Structural changes and picosecond to second dynamics of cytochrome c in interaction with nitric oxide in ferrous and ferric redox states. *Phys. Chem. Chem. Phys.* **2017**, *19*, 21317−21334.
(7) Vos, M. H.; Liebl, U. Time-resolved infrared spectroscopic studies of ligand dynamics in the active site from cytochrome c oxidase. *Biochim. Biophys. Acta, Bioenerg.* **2015**, *1847*, 79−85.
(8) Hargrove, M. S. A Flash Photolysis Method to Characterize Hexacoordinate Hemoglobin Kinetics. *Biophys. J.* **2000**, *79*, 2733−2738.
(9) Hvitved, A. N.; Trent, J. T.; Premer, S. A.; Hargrove, M. S. Ligand Binding and Hexacoordination in SynechocystisHemoglobin. *J. Biol. Chem.* **2001**, *276*, 34714−34721.
(10) Kriegl, J. M.; Bhattacharyya, A. J.; Nienhaus, K.; Deng, P.; Minkow, O.; Nienhaus, G. U. Ligand binding and protein dynamics in neuroglobin. *Proc. Natl. Acad. Sci. U. S. A.* **2002**, *99*, 7992−7997.
(11) Trent, J. T.; Watts, R. A.; Hargrove, M. S. Human Neuroglobin, a Hexacoordinate Hemoglobin That Reversibly Binds Oxygen. *J. Biol. Chem.* **2001**, *276*, 30106−30110.
(12) Puranik, M.; Nielsen, S. B.; Youn, H.; Hvitved, A. N.; Bourassa, J. L.; Case, M. A.; Tengroth, C.; Balakrishnan, G.; Thorsteinsson, M. V.; Groves, J. T.; McLendon, G. L.; Roberts, G. P.; Olson, J. S.; Spiro, T. G. Dynamics of Carbon Monoxide Binding to CooA. *J. Biol. Chem.* **2004**, *279*, 21096−21108.
(13) Gonzalez, G.; Dioum, E. M.; Bertolucci, C. M.; Tomita, T.; Ikeda-Saito, M.; Cheesman, M. R.; Watmough, N. J.; Gilles-Gonzalez, M.-A. Nature of the Displaceable Heme-Axial Residue in the EcDos Protein, a Heme-Based Sensor from Escherichia coli. *Biochemistry* **2002**, *41*, 8414−8421.
(14) Jongeward, K. A.; Magde, D.; Taube, D. J.; Traylor, T. G. Picosecond kinetics of cytochromes b5 and c. *J. Biol. Chem.* **1988**, *263*, 6027−6030.
(15) Kumazaki, S.; Nakajima, H.; Sakaguchi, T.; Nakagawa, E.; Shinohara, H.; Yoshihara, K.; Aono, S. Dissociation and Recombination between Ligands and Heme in a CO-sensing Transcriptional Activator CooA: A FLASH PHOTOLYSIS STUDY. *J. Biol. Chem.* **2000**, *275*, 38378−38383.
(16) Negrerie, M.; Cianetti, S.; Vos, M. H.; Martin, J.-L.; Kruglik, S. G. Ultrafast Heme Dynamics in Ferrous versus Ferric Cytochrome c Studied by Time-Resolved Resonance Raman and Transient Absorption Spectroscopy. *J. Phys. Chem. B* **2006**, *110*, 12766−12781.
(17) Wang, W.; Ye, X.; Demidov, A. A.; Rosca, F.; Sjodin, T.; Cao, W.; Sheeran, M.; Champion, P. M. Femtosecond Multicolor Pump-Probe Spectroscopy of Ferrous Cytochromec†. *J. Phys. Chem. B* **2000**, *104*, 10789−10801.
(18) Vos, M. H.; Battistoni, A.; Lechauve, C.; Marden, M. C.; Kiger, L.; Desbois, A.; Pilet, E.; de Rosny, E.; Liebl, U. Ultrafast Heme-Residue Bond Formation in Six-Coordinate Heme Proteins: Implications for Functional Ligand Exchange. *Biochemistry* **2008**, *47*, 5718−5723.
(19) Lim, M.; Jackson, T. A.; Anfinrud, P. A. Femtosecond Near-IR Absorbance Study of Photoexcited Myoglobin: Dynamics of Electronic and Thermal Relaxation. *J. Phys. Chem.* **1996**, *100*, 12043−12051.
(20) Ye, X.; Demidov, A.; Rosca, F.; Wang, W.; Kumar, A.; Ionascu, D.; Zhu, L.; Barrick, D.; Wharton, D.; Champion, P. M. Investigations of Heme Protein Absorption Line Shapes, Vibrational Relaxation, and Resonance Raman Scattering on Ultrafast Time Scales. *J. Phys. Chem. A* **2003**, *107*, 8156−8165.
(21) Petrich, J. W.; Poyart, C.; Martin, J.-L. Photophysics and reactivity of heme proteins: a femtosecond absorption study of hemoglobin, myoglobin, and protoheme. *Biochemistry* **1988**, *27*, 4049−4060.
(22) Cianetti, S.; Négrerie, M.; Vos, M. H.; Martin, J.-L.; Kruglik, S. G. Photodissociation of Heme Distal Methionine in Ferrous Cytochrome c Revealed by Subpicosecond Time-Resolved Resonance Raman Spectroscopy. *J. Am. Chem. Soc.* **2004**, *126*, 13932−13933.
(23) Yoshizawa, M.; Hattori, Y.; Kobayashi, T. Femtosecond time-resolved resonance Raman gain spectroscopy in polydiacetylene. *Phys. Rev. B: Condens. Matter Mater. Phys.* **1994**, *49*, 13259−13262.
(24) Kukura, P.; McCamant, D. W.; Mathies, R. A. Femtosecond Stimulated Raman Spectroscopy. *Annu. Rev. Phys. Chem.* **2007**, *58*, 461−488.
(25) McCamant, D. W.; Kukura, P.; Yoon, S.; Mathies, R. A. Femtosecond broadband stimulated Raman spectroscopy: Apparatus and methods. *Rev. Sci. Instrum.* **2004**, *75*, 4971−4980.
(26) Champion, P. M. Following the Flow of Energy in Biomolecules. *Science* **2005**, *310*, 980−982.
(27) Mukamel, S.; Biggs, J. D. Communication: Comment on the effective temporal and spectral resolution of impulsive stimulated Raman signals. *J. Chem. Phys.* **2011**, *134*, 161101.
(28) McCamant, D. W. Re-Evaluation of Rhodopsin's Relaxation Kinetics Determined from Femtosecond Stimulated Raman Lineshapes. *J. Phys. Chem. B* **2011**, *115*, 9299−9305.
(29) Batignani, G.; Fumero, G.; Mukamel, S.; Scopigno, T. Energy flow between spectral components in 2D Broadband Stimulated Raman Spectroscopy. *Phys. Chem. Chem. Phys.* **2015**, *17*, 10454−10461.
(30) Fumero, G.; Batignani, G.; Dorfman, K. E.; Mukamel, S.; Scopigno, T. On the Resolution Limit of Femtosecond Stimulated Raman Spectroscopy: Modelling Fifth-Order Signals with Overlapping Pulses. *ChemPhysChem* **2015**, *16*, 3438−3443.
(31) Batignani, G.; Fumero, G.; Pontecorvo, E.; Ferrante, C.; Mukamel, S.; Scopigno, T. Genuine dynamics vs cross phase modulation artefacts in Femtosecond Stimulated Raman Spectroscopy. *ACS Photonics* **2019**, *6*, 492−500.
(32) Pontecorvo, E.; Kapetanaki, S.; Badioli, M.; Brida, D.; Marangoni, M.; Cerullo, G.; Scopigno, T. Femtosecond stimulated Raman spectrometer in the 320−520nm range. *Opt. Express* **2011**, *19*, 1107−1112.
(33) Hoffman, D. P.; Valley, D.; Ellis, S. R.; Creelman, M.; Mathies, R. A. Optimally shaped narrowband picosecond pulses for femtosecond stimulated Raman spectroscopy. *Opt. Express* **2013**, *21*, 21685.
(34) Fang, C.; Frontiera, R. R.; Tran, R.; Mathies, R. A. Mapping GFP structure evolution during proton transfer with femtosecond Raman spectroscopy. *Nature* **2009**, *462*, 200−204.
(35) Kuramochi, H.; Takeuchi, S.; Tahara, T. Ultrafast Structural Evolution of Photoactive Yellow Protein Chromophore Revealed by Ultraviolet Resonance Femtosecond Stimulated Raman Spectroscopy. *J. Phys. Chem. Lett.* **2012**, *3*, 2025−2029.
(36) Dobryakov, A. L.; Ioffe, I.; Granovsky, A. A.; Ernsting, N. P.; Kovalenko, S. A. Femtosecond Raman spectra of cis-stilbene and trans-stilbene with isotopomers in solution. *J. Chem. Phys.* **2012**, *137*, 244505.
(37) Batignani, G.; Bossini, D.; Palo, N. D.; Ferrante, C.; Pontecorvo, E.; Cerullo, G.; Kimel, A.; Scopigno, T. Probing ultrafast photo-induced dynamics of the exchange energy in a Heisenberg antiferromagnet. *Nat. Photonics* **2015**, *9*, 506−510.
(38) Zhou, J.; Yu, W.; Bragg, A. E. Structural relaxation of photoexcited quaterthiophenes probed with vibrational specificity. *J. Phys. Chem. Lett.* **2015**, *6*, 3496.
(39) Batignani, G.; Pontecorvo, E.; Ferrante, C.; Aschi, M.; Elles, C. G.; Scopigno, T. Visualizing Excited-State Dynamics of a Diaryl Thiophene: Femtosecond Stimulated Raman Scattering as a Probe of Conjugated Molecules. *J. Phys. Chem. Lett.* **2016**, *7*, 2981−2988.
(40) Batignani, G.; Pontecorvo, E.; Bossini, D.; Ferrante, C.; Fumero, G.; Cerullo, G.; Mukamel, S.; Scopigno, T. Modeling the Ultrafast Response of Two-Magnon Raman Excitations in Antiferromagnets on the Femtosecond Timescale. *Ann. Phys.* **2019**, *531*, 1900439.

https://dx.doi.org/10.1021/jacs.9b10560
J. Am. Chem. Soc. 2020, 142, 2285−2292

(41) Batignani, G.; Pontecorvo, E.; Giovannetti, G.; Ferrante, C.; Fumero, G.; Scopigno, T. Electronic resonances in broadband stimulated Raman spectroscopy. *Sci. Rep.* **2016**, *6*, srep18445.
(42) Ferrante, C.; Pontecorvo, E.; Cerullo, G.; Vos, M. H.; Scopigno, T. Direct observation of subpicosecond vibrational dynamics in photoexcited myoglobin. *Nat. Chem.* **2016**, *8*, 1137−1143.
(43) Pontecorvo, E.; Ferrante, C.; Elles, C. G.; Scopigno, T. Spectrally tailored narrowband pulses for femtosecond stimulated Raman spectroscopy in the range 330−750 nm. *Opt. Express* **2013**, *21*, 6866−6872.
(44) Burmester, T.; Weich, B.; Reinhardt, S.; Hankeln, T. A vertebrate globin expressed in the brain. *Nature* **2000**, *407*, 520−523.
(45) Schonhoff, C. M.; Gaston, B.; Mannick, J. B. Nitrosylation of Cytochrome c during Apoptosis. *J. Biol. Chem.* **2003**, *278*, 18265−18270.
(46) Kapetanaki, S. M.; Silkstone, G.; Husu, I.; Liebl, U.; Wilson, M. T.; Vos, M. H. Interaction of Carbon Monoxide with the Apoptosis-Inducing Cytochromec-Cardiolipin Complex†. *Biochemistry* **2009**, *48*, 1613−1619.
(47) Wong, C. F.; Zheng, C.; Shen, J.; McCammon, J. A.; Wolynes, P. G. Cytochrome c: a molecular proving ground for computer simulations. *J. Phys. Chem.* **1993**, *97*, 3100−3110.
(48) Louie, G. V.; Brayer, G. D. High-resolution refinement of yeast iso-1-cytochrome c and comparisons with other eukaryotic cytochromes c. *J. Mol. Biol.* **1990**, *214*, 527−555.
(49) Silkstone, G.; Jasaitis, A.; Wilson, M. T.; Vos, M. H. Ligand Dynamics in an Electron Transfer Protein. *J. Biol. Chem.* **2007**, *282*, 1638−1649.
(50) Bowman, S. E. J.; Bren, K. L. The chemistry and biochemistry of heme c: functional bases for covalent attachment. *Nat. Prod. Rep.* **2008**, *25*, 1118.
(51) Ye, X.; Demidov, A.; Champion, P. M. Measurements of the Photodissociation Quantum Yields of MbNO and MbO2and the Vibrational Relaxation of the Six-Coordinate Heme Species. *J. Am. Chem. Soc.* **2002**, *124*, 5914−5924.
(52) Lambry, J.-C.; Vos, M. H.; Martin, J.-L. Excited State Coherent Vibrational Motion in Deoxymyoglobin. *J. Chin. Chem. Soc.* **2000**, *47*, 765−768.
(53) Wang, Q.; Wong, C. F.; Rabitz, H. Simulating Energy Flow in Biomolecules: Application to Tuna Cytochrome c. *Biophys. J.* **1998**, *75*, 60−69.
(54) Yamashita, T.; Bouzhir-Sima, L.; Lambry, J.-C.; Liebl, U.; Vos, M. H. Ligand Dynamics and Early Signaling Events in the Heme Domain of the Sensor Protein Dos fromEscherichia coli. *J. Biol. Chem.* **2008**, *283*, 2344−2352.
(55) Vos, M. H.; Reeder, B. J.; Daldal, F.; Liebl, U. Ultrafast photochemistry of the bc1 complex. *Phys. Chem. Chem. Phys.* **2017**, *19*, 6807−6813.
(56) Benabbas, A.; Champion, P. M. Adiabatic Ligand Binding in Heme Proteins: Ultrafast Kinetics of Methionine Rebinding in Ferrous Cytochrome c. *J. Phys. Chem. B* **2018**, *122*, 11431−11439.
(57) Franzen, S.; Bohn, B.; Poyart, C.; Martin, J. L. Evidence for sub-picosecond heme doming in hemoglobin and myoglobin: a time-resolved resonance Raman comparison of carbonmonoxy and deoxy species. *Biochemistry* **1995**, *34*, 1224−1237.
(58) Sun, Y.; Benabbas, A.; Zeng, W.; Kleingardner, J. G.; Bren, K. L.; Champion, P. M. Investigations of heme distortion, low-frequency vibrational excitations, and electron transfer in cytochrome c. *Proc. Natl. Acad. Sci. U. S. A.* **2014**, *111*, 6570−6575.
(59) Bu, L.; Straub, J. E. Vibrational Energy Relaxation of "Tailored" Hemes in Myoglobin Following Ligand Photolysis Supports Energy Funneling Mechanism of Heme "Cooling". *J. Phys. Chem. B* **2003**, *107*, 10634−10639.
(60) Fujisaki, H.; Straub, J. E. Vibrational energy relaxation in proteins. *Proc. Natl. Acad. Sci. U. S. A.* **2005**, *102*, 6726−6731.
(61) Agbo, J. K.; Xu, Y.; Zhang, P.; Straub, J. E.; Leitner, D. M. Vibrational energy flow across heme−cytochrome c and cytochrome c−water interfaces. *Theor. Chem. Acc.* **2014**, *133*, 1504.
(62) Bu, L.; Straub, J. E. Simulating Vibrational Energy Flow in Proteins: Relaxation Rate and Mechanism for Heme Cooling in Cytochrome c. *J. Phys. Chem. B* **2003**, *107*, 12339−12345.
(63) Arcovito, A.; Benfatto, M.; Cianci, M.; Hasnain, S. S.; Nienhaus, K.; Nienhaus, G. U.; Savino, C.; Strange, R. W.; Vallone, B.; Della Longa, S. X-ray structure analysis of a metalloprotein with enhanced active-site resolution using in situ x-ray absorption near edge structure spectroscopy. *Proc. Natl. Acad. Sci. U. S. A.* **2007**, *104*, 6211−6216.
(64) Ferrante, C.; Batignani, G.; Fumero, G.; Pontecorvo, E.; Virga, A.; Montemiglio, L. C.; Cerullo, G.; Vos, M. H.; Scopigno, T. Resonant broadband stimulated Raman scattering in myoglobin. *J. Raman Spectrosc.* **2018**, *49*, 913−920.
(65) Batignani, G.; Ferrante, C.; Fumero, G.; Scopigno, T. Broadband impulsive stimulated Raman scattering based on a chirped detection. *J. Phys. Chem. Lett.* **2019**, *10*, 7789−7796.
(66) Agrawal, G. *Nonlinear Fiber Optics*; Academic Press: London, 2013.

https://dx.doi.org/10.1021/jacs.9b10560
J. Am. Chem. Soc. 2020, 142, 2285−2292